

# MODELLING DYNAMICAL CORRELATION FORCES IN LOW-ENERGY POSITRON SCATTERING FROM POLYATOMIC GASES: A COMPARISON FOR CH<sub>4</sub>

F.A. Gianturco<sup>+\*</sup>, T.L. Gibson<sup>\*</sup>, P. Nichols<sup>\*</sup>, R.R. Lucchese<sup>°</sup>, T. Nishimura<sup>+</sup>

<sup>+</sup> *Department of Chemistry and INFN, the University of Rome "La Sapienza"*

*Piazzale A. Moro 5, 00185 Rome, Italy*

<sup>\*</sup> *Department of Physics, Texas Tech. University*

*P.O. Box 4180, Lubbock, TX 79409-1051, USA*

<sup>°</sup> *Department of Chemistry, Texas A&M University*

*College Station, TX 77843-3255, USA*

(August 1, 2002)

## Abstract

Two different models for treating the contributions of dynamical electron-positron correlation forces to the full interaction between low-energy positron beams scattered off polyatomic gases are considered and applied to obtain the elastic integral and differential cross sections (at collision energies below Ps formation) for the methane molecule. The computed quantities are then compared with available experiments, both for integral and differential data, and found to be in good accord with measured quantities. Both models also agree rather closely with each other and the physical reasons for this behavior are briefly discussed.

---

\*corresponding author. E.mail: fa.gianturco@caspur.it. Fax: +39-06-49913305

## I. INTRODUCTION

The interaction of low-energy positron and positronium (Ps) beams with atomic and molecular gases has attracted increasing attention in recent years because of the wide range of good-quality experiments that has become available and because of the testing of the more fundamental properties of atoms and molecules which have become accessible as the beam energies have gone down to the thermal or near-thermal range while also increasing their intensity. Thus, one finds that this particular leptonic particle is providing very interesting probes of elementary forces, of microscopic structures and of fundamental processes that can occur in atomic and molecular gases (See for example Surko and Gianturco, 2002). As the quality of the experiments improves, however, and as the range of probed molecular gases increases with them (Gilbert *et al.*, 1999; Kawada *et al.*, 2000; Laricchia and Wilkin, 1997), the demands on more realistic physical models for the processes which are being observed are also increasing and therefore better quality computational treatments become vital for providing realistic interpretations of, and good agreement with, the broad variety of data gathered on a very large class of molecular systems. This is especially true when one is dealing with more complicated molecules, made up of several different atoms and a large number of bound electrons, which tremendously increase, with their higher density of internal states, the complexity of treating as correctly as possible the dynamical couplings between the impinging, slow positron and the bound, electronuclear molecular “network”.

We have endeavored, over the years, to put together a parameter-free modelling of the forces at play in several examples of polyatomic targets (Gianturco and Mukherjee, 1999; Curik *et al.*, 2000; Gianturco and Mukherjee, 2001; Gianturco *et al.*, 2001; Nishimura and Gianturco, 2002) undergoing elastic, inelastic scattering and annihilation processes with slow positron beams. In all the cases examined it turned out that the modelling of the short-range correlation forces, which evolve into the long-range (LR) polarization interaction once the positron is well outside the molecular charge distribution, is one of the crucial ingredients for a realistic treatment of scattering observables. In the present study we

therefore analyze in some details two different ways of obtaining what goes under the name of the correlation-polarization potential for positron scattering,  $V_{\text{cp}}$ . The latter quantity should rigorously be a nonlocal, energy-dependent interaction potential (see for example van Rieth and Humbertson, 1998) since it is meant to describe the response function of the bound electron density to the dynamical distortion induced by the travelling, continuum positron projectile during the time of its overlapping interaction with the electronuclear molecular network. However, the problem is already simplified at the outset by separating the nuclear motion and describing the  $e^- - e^+$  correlation effects within a Born-Oppenheimer picture for the molecular nuclei which are usually considered as frozen in a given geometry during the scattering process. This approximation is known as the fixed-nuclei approximation (FN) (see for example Kimura *et al.*, 1998). Further simplifications need to be introduced depending on the collision energy region one wishes to consider and on the dynamical observable one wants to evaluate for experimental comparison. In the following Section we will therefore describe two of the modelling approaches that we have considered for an efficient and realistic handling of polyatomic gases, and for which we will show a specific application and comparison in Section III. Our conclusions will be briefly summarized in Section IV.

## II. THE POSITRON-MOLECULE SCATTERING EQUATIONS

As mentioned in the Introduction, we represent the interaction potential between the impinging positron and the molecular target with a local form. It contains contributions from the electrostatic interaction of  $e^+$  with the molecular nuclei (kept at their fixed equilibrium geometry) and the bound molecular electrons plus the correlation effects from the short-range dynamical couplings between the bound electrons and the positron,  $V_{\text{corr}}$ , that evolve in the LR region of large  $e^+$ -molecule distances into the dipole polarization potential  $V_{\text{pol}}$ . The object of the present study is to show the different ways in which the correlation-polarization potential,  $V_{\text{cp}} = V_{\text{corr}} + V_{\text{pol}}$ , can be obtained for a polyatomic target and what the consequences are in the calculation of the scattering attributes that can be compared

with experiments such as angular distributions at low scattering energies and integral cross sections below the Ps formation threshold, which is 5.8 eV for the CH<sub>4</sub> target.

### A. Single Center Expansion Equations

In our approach any three-dimensional function, being either one of the bound state orbitals  $\phi_i(\mathbf{r}_i)$  for one of the  $N$  bound electrons or the wave function  $\psi(\mathbf{r})$  describing the impinging positron, is expanded using a single-center expansion (SCE) about the center-of-mass of the molecule (Gianturco and Jain, 1986)

$$\phi_i^{p_i\mu_i}(\mathbf{r}_i) = \frac{1}{r_i} \sum_{l,h} u_{ilh}^{p_i\mu_i}(r_i) X_{lh}^{p_i\mu_i}(\hat{r}_i), \quad (1)$$

$$\psi^{p\mu}(\mathbf{r}_p) = \frac{1}{r_p} \sum_{l,h} \psi_{lh}^{p\mu}(r_p) X_{lh}^{p\mu}(\hat{r}_p), \quad (2)$$

where  $i$  labels a specific, multicenter occupied orbital, which belongs to the specific irreducible representation (IR) of the point group of the molecule. The indices  $p$  and  $\mu$  label a relevant IR  $p$  and one of its components  $\mu$ . The index  $h$  labels a specific basis, for a given partial wave  $l$ , used within the  $\mu$ th component of the  $p$ th IR. The symmetry-adapted angular functions in eqs. (1) and (2) are defined by

$$X_{lh}^{p\mu}(\hat{r}) = \sum_m b_{lmh}^{p\mu} Y_{lm}(\hat{r}). \quad (3)$$

The details about the computation of the transformation matrices  $b_{lmh}^{p\mu}$  have been given before and will not be repeated here (Gianturco and Jain, 1986).

One of the two methods for finding the solutions of the scattering equations which we employ is essentially that given by Sams and Kouri (1969a; 1969b) and further extended by Rescigno and Orel (1981).

The interaction potential can be generally written in a local form  $V_{\text{loc}}(\mathbf{r}_p)$  (here the static and correlation-polarization potentials) for a slow positron-molecule collision. The SCE method expansion then results in the following set of radial differential equations:

$$\left[ \frac{d^2}{dr^2} - \frac{l_i(l_i + 1)}{r_p^2} + k^2 \right] \psi_{ij}^{p_i\mu_i}(r_p) = 2 \sum_n \left[ V_{in}(r_p) \psi_{nj}^{p_n\mu_n}(r_p) \right], \quad (4)$$

where indices  $i, j, n$  represent pairs of angular channel indices  $(l, h)$ . The local potential matrix elements are

$$V_{in}(r_p) = \langle X_i^{p\mu}(\hat{r}_p) | V_{\text{loc}}(\mathbf{r}_p) | X_n^{p\mu}(\hat{r}_p) \rangle = \int d\hat{r}_p [X_i^{p\mu}(\hat{r}_p)]^* V_{\text{loc}}(\mathbf{r}_p) X_n^{p\mu}(\hat{r}_p). \quad (5)$$

The non diverging solutions of eq. (4) satisfy its integral form (where for simplicity we omit the  $(p\mu)$  labels)

$$\psi_{ij}(r_p) = \delta_{ij} j_l(kr_p) + 2 \sum_n \int_0^\infty dr'_p j_l(kr_{p,<}) n_l(kr_{p,>}) V_{in}(r'_p) \psi_{nj}(r'_p), \quad (6)$$

where  $j_l(kr)$  and  $n_l(kr)$  are Riccati-Bessel and Riccati-Neumann functions. One can show that  $\psi_{ij}(r_p)$  can also be obtain from

$$\psi_{ij}(r_p) = \sum_{n=1}^{n_{\text{max}}} \psi_{in}^0(r_p) C_{nj}, \quad (7)$$

where the  $n_{\text{max}}$  wave functions on the right-hand side of eq. (7) satisfy the following set of  $n_{\text{max}}$  Volterra equations (for the detailed derivation see Sams and Kouri (1969a; 1969b) and Rescigno and Orel (1981))

$$\psi_{ij}^0(r_p) = \delta_{ij} j_l(kr_p) + 2 \sum_n \int_0^{r_p} dr'_p g_l(r_p, r'_p) V_{in}(r'_p) \psi_{nj}^0(r'_p), \quad (8)$$

with

$$g_l(r_p, r'_p) = \frac{1}{k} \left[ j_l(kr_p) n_l(kr'_p) - n_l(kr_p) j_l(kr'_p) \right]. \quad (9)$$

One should note here that the above approach is chosen because of its numerical simplicity, although the more common use of ordinary differential equation solution methods is just as viable an alternative and we have also employed it in the present study, as described in detail in our earlier work (Gianturco and Lucchese, 1999).

The model local interaction potential,  $V_{\text{loc}}(\mathbf{r}_p)$ , can be written as

$$V_{\text{loc}}(\mathbf{r}_p) = V_{\text{st}}(\mathbf{r}_p) + V_{\text{cp}}(\mathbf{r}_p), \quad (10)$$

where the static potential  $V_{\text{st}}$  for closed-shell molecule with  $N_{\text{occ}}$  doubly occupied orbitals and  $M$  nuclear centers takes the form

$$V_{\text{st}}(\mathbf{r}_p) = \sum_{a=1}^M \frac{Z_a}{|\mathbf{r}_p - \mathbf{R}_a|} - 2 \sum_{i=1}^{N_{\text{occ}}} \int d^3r' \frac{|\phi_i(\mathbf{r}')|^2}{|\mathbf{r}_p - \mathbf{r}'|}. \quad (11)$$

The well known physical shortcoming of limiting the local interaction in eq. (10) to the  $V_{\text{st}}$  contribution only is the omission of the all-important target response function, *i. e.* the effects from the dynamical correlation between the continuum lepton  $e^+$  and the bound target electrons below the scattering energy required for Ps formation. Such forces will change over, outside the region of overlap between the bound electrons and the continuum function, to the LR polarization forces chiefly described by the dipole polarizability contribution

$$V_{\text{pol}}(r_p)_{r_p \rightarrow \infty} \sim -\frac{\alpha}{2r_p^4}. \quad (12)$$

Strictly speaking, this effect arises as virtual excitations of energetically closed electronic states, including continuum ones. In practice, however, the infinity of such states precludes treating polarization rigorously. Considerable effort has therefore been expended in the past three decades to try to include it as accurately as possible, albeit not rigorously. In addition, what makes computational treatments so difficult is not only the representation of the distortion of the target electron density as a function of a charge fixed some distance away from the origin of all charges, but also the additional effects which come to play near and within the target core mentioned before. Moreover, a further complication comes from when the wave function of the incident particle strongly overlaps the target core, the independent-particle model breaks down and many-body effects predominate. In order to devise simpler ways of handling the polarization forces over the whole range of relative distances, various approaches have been tried in recent years, as discussed in Gianturco and Lucchese (1999) and Gianturco *et al.* (2001). Ideally, such model correlation-polarization potentials ( $V_{\text{cp}}$ ) should be free of empirical parameters which need adjustment to experimental cross sections, and it is in this sense that they are often described as *ab initio* potentials. As for the positron projectile, the absence of some nonlocal effects such as the electron exchange should make the treatment of its low-energy scattering from many-electron targets less difficult and computationally less demanding. The  $V_{\text{st}}$  can be treated exactly and therefore the way one

handles the  $V_{cp}$  plays an essential role in deciding on the quality of the theoretical model. At large distances from the core, the velocity of positron can be considered low enough so that the bound electrons respond adiabatically to the positron without specific dependence on its local velocity. As the incident positron nears the target, however, the repulsive Coulomb core further slows it down while the attraction from the bound electrons increases and strongly modifies its motion in the intermediate region via a correlation process similar to multiple-scattering effects. The  $V_{cp}$  at short-range (SR) is therefore not only collision energy dependent but also nonlocal. As a result, in regions of intermediate- and SR interactions, nonadiabatic nonlocal effects play an important role and differences appear between the behavior of electron and positron as projectiles (Gianturco *et al.*, 1993).

A simple remedy has been to multiply eq. (12) by a cutoff function involving some adjustable parameter. Nevertheless, this approach is unsatisfactory, although the results may be "tuned" to agree with observations. For positron scattering, most of the calculations prior to 1990 used a  $V_{cp}$  which was the one employed for electron scattering,  $V_{ecp}$ , assuming that such distortion effects are not sensitive to the sign of the charge of projectile, and agree with the experiment well (see for example Gianturco *et al.*, 1993). Morrison *et al.* (1984), on the other hand, found that the  $V_{ecp}$  is inadequate and that there is a need to generate a true positron polarization potential, a more correct  $V_{cp}$  potential.

## B. The Positron-Electron Correlation-Polarization Model

The first of our present  $V_{cp}$  models, the  $V_{p_{cp}}$  potential, was first applied to positron scattering (Jain, 1990; Jain and Gianturco, 1991) and is based on the correlation energy  $\varepsilon^{e-p}$  of a localized positron in an electron gas together with its hybridization to the correct asymptotic form of eq. (12). The quantity  $\varepsilon^{e-p}$  has been originally derived by Arponen and Pajanne (1975; 1979) from the theory that the incoming positron is assumed to be a charged impurity at each fixed distance  $\mathbf{r}_p$  in an homogeneous electron gas which is in turn treated as a set of interacting bosons which represent the collective excitations within the usage of

the random phase approximation. Based on their work, Boronski and Nieminen (1986) gave the interpolation formulae of  $\varepsilon^{\varepsilon^{-p}}$  over the entire range of the density parameter  $r_s$  which satisfies the relationship of  $\frac{4}{3}\pi r_s^3 \rho(\mathbf{r}) = 1$ . The relationship between the  $V_{\text{corr}}$  and  $\varepsilon^{\varepsilon^{-p}}$  which is consistent with the local density approximation and a variational principle for a total collision system with the size of the target is given by (Kohn and Sham 1965a; 1965b)

$$V_{\text{corr}}(\mathbf{r}_p) = \frac{d}{d\rho} \left\{ \rho(\mathbf{r}_p) \varepsilon^{\varepsilon^{-p}}[\rho(\mathbf{r}_p)] \right\}, \quad (13)$$

where  $\rho$  denotes the undistorted electronic density of the target, and this quantity provides the probability for finding any of the electrons near the impinging positron. Thus, the total  $V_{\text{pcp}}$  potential for the  $e^+$ -molecule system is given by

$$\begin{aligned} V_{\text{pcp}}(\mathbf{r}_p) &= V_{\text{corr}}(\mathbf{r}_p) \quad \text{for } r_p < r_c, \\ &= V_{\text{pol}}(\mathbf{r}_p) \quad \text{for } r_p > r_c. \end{aligned} \quad (14)$$

The  $V_{\text{corr}}$  is connected with the asymptotic form of eq. (12) at the position of  $r_c$  (say, around a few  $a_0$ ) where  $V_{\text{corr}}$  and  $V_{\text{pol}}$  first cross each other as  $r_p$  increases. In our present case of  $\text{CH}_4$ , the value for  $r_c$  is  $3.2 a_0$ .

The total local interaction potential,  $V_{\text{loc}}$ , as defined in eq. (10) is therefore given by the sum of the exact static interaction between the impinging positron and the (electrons and nuclei) components of the molecular target  $V_{\text{st}}$  (for detail forms, see for example Gianturco and Jain, 1986) and the  $V_{\text{pcp}}$ .

### C. The Distributed Positron Model

Another possible model correlation-polarization potential which can be used to model  $V_{\text{cp}}$  in eq. (10) is the distributed positron model (DPM) potential,  $V_{\text{dpm}}$ . The form adopted here for the  $V_{\text{dpm}}$ , is based on a modification of the adiabatic polarization approach which makes use of quantum chemistry technology to provide a variational estimate of the polarization potential. In the adiabatic approximation to the polarization potential, the positron is



treated as an additional “nucleus” (a point charge of +1) fixed at location  $\mathbf{r}_p$  with respect to the center of mass of the atomic or molecular target. The target electronic orbitals are allowed to relax fully in the presence of this fixed additional charge and the energy lowering due to the distortion is recorded. This energy lowering represents the adiabatic polarization potential at one point in space. Of course, in order to represent fully the spatial dependence of this interaction many such points must be computed.

However, due to nonadiabatic and SR correlation effects, e.g. virtual Ps formation, the adiabatic approximation can overestimate the strength of the polarization potential for smaller values of  $r_p$  where the positron has penetrated the target electronic cloud. The present  $V_{\text{dpm}}$  corrects for this by treating the positron as a smeared out distribution of charge rather than as a point charge. If the scattering particle really were an additional nucleus, a proton, then the dominant SR correlation effect would be virtual hydrogen atom formation into ground and excited states, and the delta function distribution of positive charge at the center of mass would be correct. But, for a Ps atom, the positive charge is not localized at the center of mass and to mimic this effect in computing the polarization potential we represent the positron as a spherical distribution of charge. This leads to a polarization potential that more closely reflects the correct physics and that smoothly reduces to the expected result for larger values of  $r_p$ .

The distortion of the molecular orbitals in the electronic structure code employed here is driven by the nuclear attraction integrals (NAIs) that involve the positron,

$$I_{ij}^{\text{NAI}} = \langle \alpha_i(\mathbf{r}_e) | V(\mathbf{r}_e; \rho_{\text{pos}}) | \beta_j(\mathbf{r}_e) \rangle \quad (15)$$

where the interaction  $V$  between an electron and  $\rho_{\text{pos}}$  is given by

$$V(\mathbf{r}_e; \rho_{\text{pos}}) = \int d^3r_p \rho_{\text{pos}}(\mathbf{r}_p) \frac{-1}{|\mathbf{r}_e - \mathbf{r}_p|} \quad (16)$$

For the adiabatic approximation, we have  $\rho_{\text{pos}}(\mathbf{r}_p) = \delta^3(\mathbf{r}_p - \mathbf{r}'_p)$ , which is appropriate for the positive charge distribution in a virtual hydrogen atom and results in the standard nuclear attraction integrals (Lucchese *et al.*, 2001). Although there is no precise data that

would allow us to fix the size of the distribution, this parameter has never been treated as a “tunable parameter”. We do not suggest that our choice of  $\rho_{\text{pos}}$  is by any means an exact representation when the virtual Ps is part of an atomic or molecular target. It is merely a physically reasonable choice that automatically reduces to the adiabatic result in the appropriate region. In earlier studies (Gibson, 1990; 1992) of positron scattering involving the  $V_{\text{dpm}}$  the choice was a convenient, uniform spherical charge distribution whose radius  $R_p$  was set to either the average ground state Ps radius of  $1.5 a_0$  or to  $1.0 a_0$ , the maximum in the ground state Ps radial distribution with respect to the Ps center of mass. Both choices provided enormous improvement over scattering results obtained with the simple adiabatic approximation and strongly suggest that the  $V_{\text{dpm}}$  mimics the correct physics for SR correlation.

As originally implemented, the  $V_{\text{dpm}}$  scheme made use of direct three dimensional quadratures in the modified nuclear attraction integrals of eq. (15) so that essentially any choice of  $\rho_{\text{pos}}$  could be accommodated. However, to implement the  $V_{\text{dpm}}$  model for larger target molecules such as  $\text{SF}_6$  (Lucchese *et al.*, 2001) we construct  $\rho_{\text{pos}}$  from the STO-3G basis for  $1s$  atomic hydrogen with Slater exponent  $\xi = 1.24$ . This choice gives results similar to those obtained with the  $V_{\text{dpm}}$  where  $r_p = 1.5 a_0$ , but has the advantage that all of the modified NAIs can be evaluated in closed form by means of the very efficient functions used to compute two-electron integrals. Once the  $V_{\text{dpm}}$  potential is calculated, it is combined with the static potential to yield the total local interaction potential of eq. (10).

### III. RESULTS AND DISCUSSION

In the  $V_{\text{pcp}}$  calculations the  $\text{CH}_4$  molecule was kept in its equilibrium geometry and  $T_d$  symmetry. The target orbitals were expanded over a set of Gaussian-type orbitals (GTOs) obtained at the D95\* level of expansion via the GAUSSIAN 98 code (Frisch *et al.*, 1998). The self-consistent field (SCF) total energy was -40.200639 hartrees. For the calculations that employed the  $V_{\text{pcp}}$  model we performed the SCE description of the five occupied MOs

by employing up to  $l_{\max} = 12$  in the multipolar coefficients, thereby constructing the corresponding static and correlation potentials up to  $\lambda_{\max} = 24$ . The numerical grid in the  $(r, \vartheta, \varphi)$  space used a  $(800 \times 56 \times 25)$  set of points, with the maximum radial value,  $r_{p,\max} = 74.14 a_0$ . The scattering calculations were then carried out using a maximum value of the positron partial wave of 12. For the calculations which employed the  $V_{\text{dpm}}$  model potential the target electrons described at the aug-cc-pVQZ quality level (Frish *et al.*, 1998), with a bond length, like before, of  $1.0837 a_0$ . The resulting SCF energy turned out to be  $-40.216489$  hartrees. The asymptotic polarizability from this model comes to be  $16.13 a_0^3$ , close to the experimental value of  $17.54 a_0^3$  employed within the  $V_{\text{pcp}}$  potential. A total of 44,030 points of the  $(r, \vartheta, \varphi)$  grid were generated to construct the  $V_{\text{dpm}}$  potential. The occupied target MOs were expanded up to  $l_{\max} = 30$  and the potential had  $\lambda_{\max} = 60$  for the  $V_{\text{st}}$  and  $\lambda_{\max} = 16$  for the  $V_{\text{dpm}}$ . The scattering calculations had a fixed radial grid out to  $r_p = 14 a_0$  using 1,408 radial points. This grid was then dynamically extended until  $V_{\text{loc}}/E_{\text{coll}} < 10^{-6}$ . Thus for example, when the collision energy,  $E_{\text{coll}}$  was 1.0 eV, the grid was extended to  $139 a_0$ . The  $(\vartheta, \varphi)$  grid was given by  $(128 \times 61)$  points. The scattered positron was expanded up to  $l_{\max} = 30$  but only  $l_{\max} = 10$  was used to construct the corresponding K-matrix. The gaussian width employed for the positron was given by an exponential value of 1.24, as discussed before and as used in earlier work (Lucchese *et al.*, 2001). The basis set used in the computation of the  $V_{\text{dpm}}$  potential was  $(6s3p)$  on the H atoms (Huzinaga, 1965; Dunning, 1971) and was  $(9s5p/4s3p)$  on the C atom (Dunning, 1970) with additional  $(2s, 1p, 2d)$  diffuse functions added.

We report in figure 1 the spherical component of the two model potential employed in the present comparison, where we see that the  $V_{\text{pcp}}$  model is definitely stronger near the core, where however the repulsive  $V_{\text{st}}$  largely dominates the scattering. However, the intermediate range of interaction shows initially a stronger effect from the  $V_{\text{pcp}}$  as compared to the weaker (and smoother)  $V_{\text{dpm}}$  treatment (for  $1.0 \leq r_p \leq 4.0 a_0$ ) but exhibits a switch of strength before merging into the “really” asymptotic region: the intermediate region between about 4.0 and about 8.0  $a_0$ , therefore, corresponds to the transition between the strongly attractive

SR core and the asymptotic LR polarization. Here the two potential models behave indeed differently but their crossings also indicate a possible compensation effect in the evaluation of the final observables from the scattering dynamics.

That this may be the case could be gleaned from the results reported in figure 2, where we show the total integral cross sections (TCS) obtained from the experiments of Sueoka and Mori (1986) (filled in circles) and then subtract from them the experimentally determined vibrationally inelastic cross sections of Sullivan *et al.* (2002), in order to obtain a better estimate of the elastic cross sections (open circles).

The computed elastic integral cross sections (ICS) are also reported in the same figure: the solid line gives the values obtained from the  $V_{\text{dpm}}$  model potential, while the dashes report the elastic (rotationally summed) ICS obtained by using the  $V_{\text{pcp}}$  potential. Both curves follow rather closely the experiments, but the  $V_{\text{dpm}}$  results are always yielding larger cross sections down to the energy region between 1.0 and 3.0 eV. The values from  $V_{\text{dpm}}$  are however larger than the measured elastic data, while the  $V_{\text{pcp}}$  results are slightly smaller. Such differences are the results of the  $V_{\text{dpm}}$  potential producing stronger interactions than the  $V_{\text{pcp}}$  in the intermediate radial range (see figure 1), where the balance between the repulsive  $V_{\text{st}}$  and the attractive  $V_{\text{cp}}$  components is most important for the final cross sections. Both model potentials, however, are seen to produce rather fair accord with the measured data and to provide an acceptable description of the forces at play.

It is well known that the angular distributions from the scattering experiments are a very sensitive test of the various features of the chosen interaction potentials. The results reported in figures 3 to 6 therefore show our computed elastic (rotationally summed) differential cross sections (DCS) at four different collision energies from 1.0 eV up to 6.0 eV. For the calculations at 4.0 and 6.0 eV (figures 5 and 6) we also report the available experimental cross sections of Przybyla *et al.* (1997), scaled to match the calculated values from the  $V_{\text{dpm}}$  potential at  $90^\circ$ . One can make the following comments from a perusal of the figures:

1. both computational models provide very similar shapes of the angular distributions

and do so at all the energies examined;

2. the calculations using the  $V_{\text{pcp}}$  potential exhibit smaller DCS values, both in the backward and forward scattering regions, when the lower collision energies are considered (figures 3 and 4). However, when we examine the higher energy distributions (figures 5 and 6), we see that the values of the backward scattering using the  $V_{\text{pcp}}$  potential become larger: the SR region of the latter, which is stronger than that of the  $V_{\text{dpm}}$  potential, is therefore playing a greater role;
3. the shape of the experimental DCS available below Ps threshold, only at 4.0 and 6.0 eV, however appears to be well reproduced by both sets of calculations, which show good agreement with the measured data by confirming the presence of a DCS minimum between  $50^\circ$  and  $60^\circ$ . Furthermore, the strong increase of the experimental values in the forward-scattering region is also reproduced reasonably well by both our computational models.

#### IV. CONCLUSIONS

In conclusion, we have seen that differences exist between the two model potentials used in the present work, but that nonetheless they both appear to yield ICS and DCS values which are very similar in value and shape and that also agree surprisingly well with the available experimental data. In other words, the possibility of treating larger polyatomic targets when studying scattering processes with positron beams at energies below the Ps formation threshold is shown by the present study to be viable through the use of model potentials for the description of the all-important correlation-polarization effects. The  $V_{\text{dpm}}$  is also seen to provide a smoother behavior of that interaction and to differ the most from the  $V_{\text{pcp}}$  potential model in the intermediate regions that connect the SR to the LR interaction values.

## V. ACKNOWLEDGEMENTS

R.R.L. Wishes to thank the Welch Foundation (Houston) for its financial support under grant no. A-1020 and to acknowledge the support of Texas A&M University Supercomputing Facility. T.L.G. and P.N. are also grateful from support from the Robert A. Welch Foundation under grant no. D-1316 and would like to thank Mr. Lee Burnside for his expertise in constructing and running the Beowulf cluster. F.A.G. and T.N. thank the Max-Planck Society for financial support of T.N. during his stay in Rome and the Italian Ministry for University and Research (MUIR) for its financial support through one of its PRIN projects.

## REFERENCES

- Arponen, J., Pajanne, E., 1975. *Ann. Phys.* 91, 450.
- Arponen, J., Pajanne, E., 1979. *Ann. Phys.* 121, 343.
- Boronski, W., Nieminen, R. M., 1986. *Phys. Rev. B* 34, 3820.
- Curik, R., Gianturco, F. A., Sanna N., 2000. *J. Phys. B* 33, 615.
- Dunning, T. H., Jr., 1970. *J. Chem. Phys.* 53, 2823.
- Dunning, T. H., Jr., 1971. *J. Chem. Phys.* 55, 3958.
- Frish, M. J. *et al.*, 1988. GAUSSIAN 98, Revision A.7, Gaussian Inc., Pittsburgh.
- Gianturco, F. A., Jain, A., 1986. *Phys. Rep.* 143, 347.
- Gianturco, F. A., Jain, A., Rodriguez-Ruiz, J. A., 1993. *Phys. Rev. A* 48, 4321.
- Gianturco, F. A., Lucchese, R. R., 1999. *Phys. Rev. A* 60, 4567.
- Gianturco, F. A., Mukherjee, T., 1999. *Europhys. Lett.* 48, 519.
- Gianturco, F. A., Mukherjee, T., 2001. *Phys. Rev. A* 64, 024703.
- Gianturco, F. A., Mukherjee, T., Nishimura, T., Occhigrossi, A., 2001. In: *New Directions in Antimatter Chemistry and Physics*, Kluwer Academic, Dordrecht, pg. 45.
- Gianturco, F. A., Mukherjee, T., Occhigrossi, A., 2001. *Phys. Rev. A* 64, 032715.
- Gibson, T. L., 1990. *J. Phys. B* 23, 767.
- Gibson, T. L., 1992. *J. Phys. B* 25, 1321.
- Gilbert, S. J., Greaves, R. G. and Surko, C. M., 1999. *Phys. Rev. Lett.* 82, 5032.
- Huzinaga, S., 1965. *J. Chem. Phys.* 42, 1293.

- Jain, A., 1990. Phys. Rev. A 41, 2437.
- Jain, A., Gianturco, F. A., 1991. J. Phys. B 24, 2387.
- Kawada, M. K., Sueoka, O., Kimura, M., 2000. J. Chem. Phys. 112, 7057.
- Kimura, M., Takekawa, M., Itikawa, Y., Takaki, H., Sueoka, O., 1998. Phys. Rev. Lett. 80, 3936.
- Kohn, W., Sham, L. J., 1965a. Phys. Rev. 137, A1697.
- Kohn, W., Sham, L. J., 1965b. Phys. Rev. 140, A1133.
- Laricchia, G., Wilkin, C., 1997. Phys. Rev. Lett. 79, 2241.
- Lucchese, R. R., Gianturco, F. A., Nichols, P., Gibson, T. L., 2001. In: New directions in Antimatter Chemistry and Physics, Surko, C.M., Gianturco, F.A. (Eds), Kluwer Academic, Dordrecht, pg. 475.
- Morrison, M. A., Gibson, T. L., Austin, D., 1984. J. Phys. B, 17, 2725.
- Morrison, M. A., Hay, P. J., 1979. Phys. Rev. A 20, 740.
- Nishimura, T., Gianturco, F. A., 2002. Phys. Rev. A 65, 062703.
- Przybyla, D. A., Kauppila, W. E., Kwan, C. K., Smith, S. J., Stein, T. S., 1997. Phys. Rev. A 55, 4244.
- Rescigno, T. N., Orel, A. E., 1981. Phys. Rev. A. 24, 1267.
- Sams, W. M., Kouri, D. J., 1969a. J. Chem. Phys. 51, 4809.
- Sams, W. M., Kouri, D. J., 1969b. J. Chem. Phys. 51, 4815.
- Sueoka, O., Mori, S., 1986. J. Phys. B 19, 4035.
- Sullivan, J. P., Gilbert, S. J., Marler, J. P., Barnes, L. D., Buckman, S. J., Surko, C. M., 2002. Nucl. Instr. Methods Phys. Res. B 192, 3.



Surko, C. M., Gianturco, F. A. (Eds.), 2002. *New Directions in Antimatter Chemistry and Physics*, Kluwer Academic Publishers, Dordrecht.

Truhlar, D. G., Dixon, D. A., Eades, R., 1979. *J. Phys. B* 12, 1913.

van Rieth, P., Humbertson, J. W., 1998. *J. Phys. B* 31, L231.

## FIGURE CAPTIONS

**Figure 1:** Computed spherical components of the  $V_{\text{dpm}}$  potential model (solid line) and the  $V_{\text{pcp}}$  potential model (dashed line) for the  $\text{CH}_4$  target. See text for further details.

**Figure 2:** Computed and measured integral cross sections (ICS) below Ps formation for  $e^+ - \text{CH}_4$  scattering. The filled circles report the total ICS values from the experiments of Sueoka and Mori (1986) which are on an absolute scale, while the open circles are the elastic ICS obtained by subtracting the inelastic contributions from Sullivan *et al.* (2002). The solid lines are calculations using the  $V_{\text{dpm}}$  potential while the dashed line report the same calculations using the  $V_{\text{pcp}}$  potential.

**Figure 3:** Computed elastic angular distributions for a collision energy of 1.0 eV. The solid line shows results using the  $V_{\text{dpm}}$  potential while the dashed are the calculations using the  $V_{\text{pcp}}$  potential.

**Figure 4:** Same as in figure 3 but for a collision energy of 2.0 eV.

**Figure 5:** Same as in figure 3 but for a collision energy of 4.0 eV. The filled circles are the scaled experimental values from Przybyla *et al.* (1997).

**Figure 6:** Same as in figure 5 but for a collision energy of 6.0 eV.

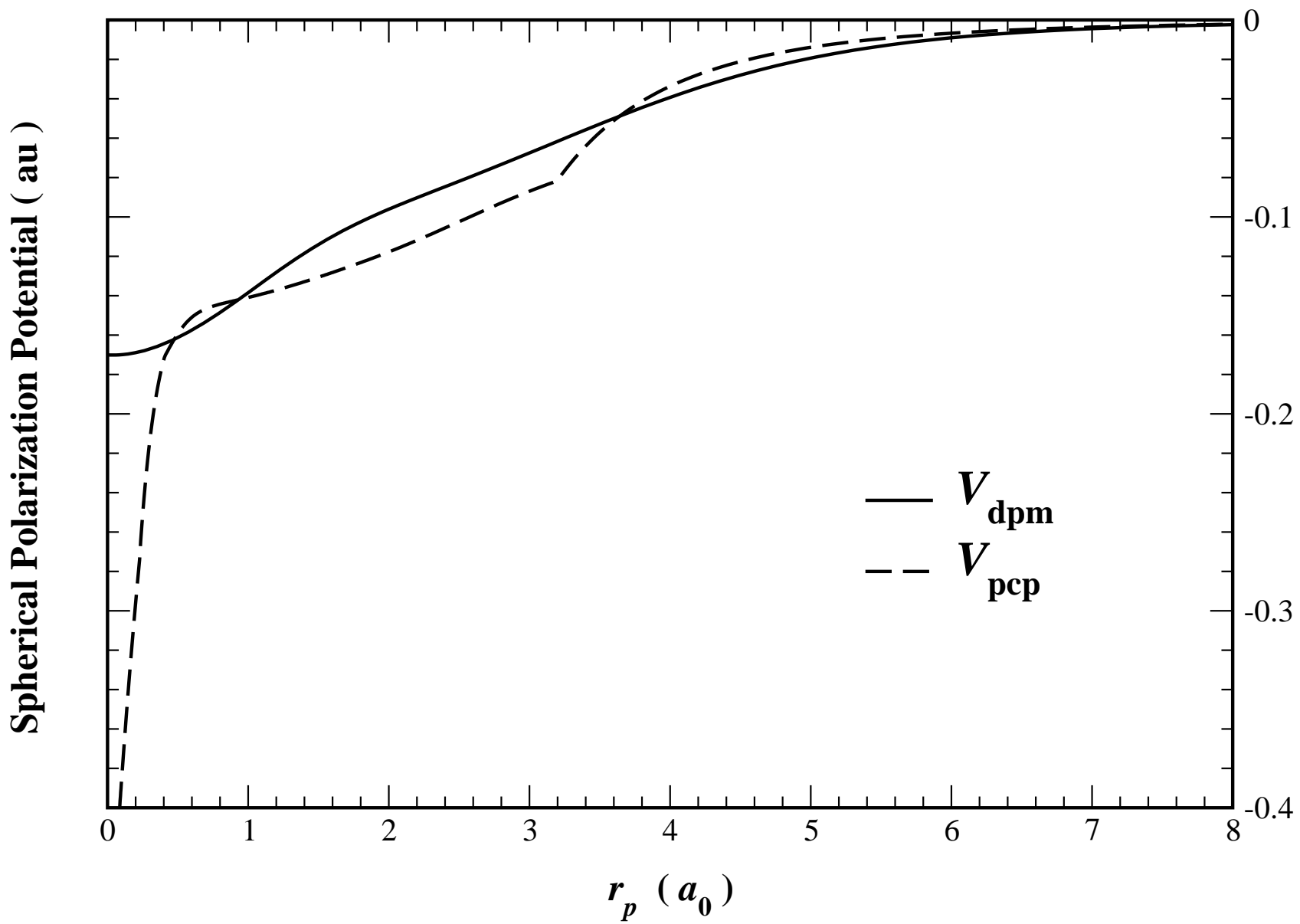


Figure 1

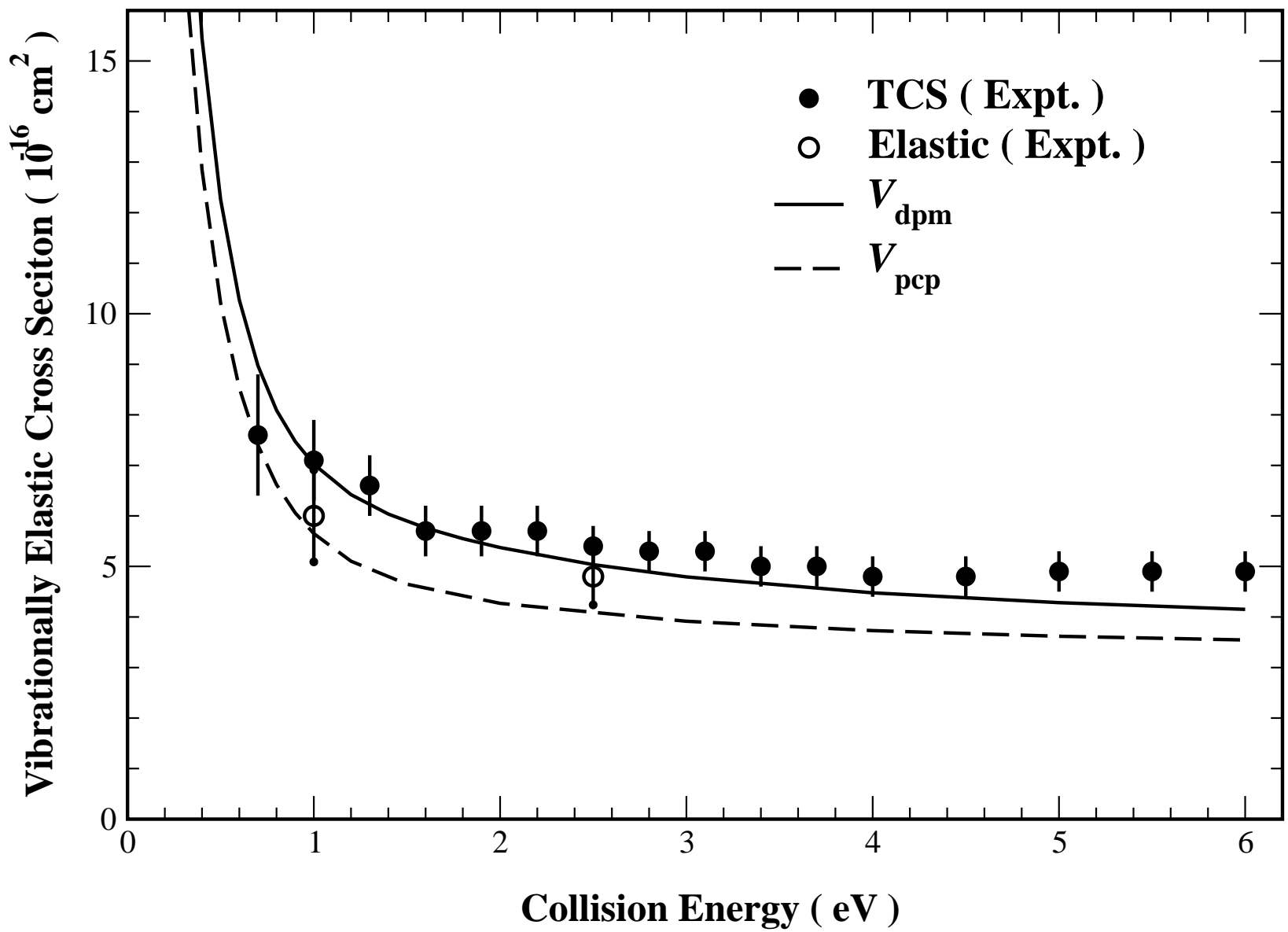


Figure 2

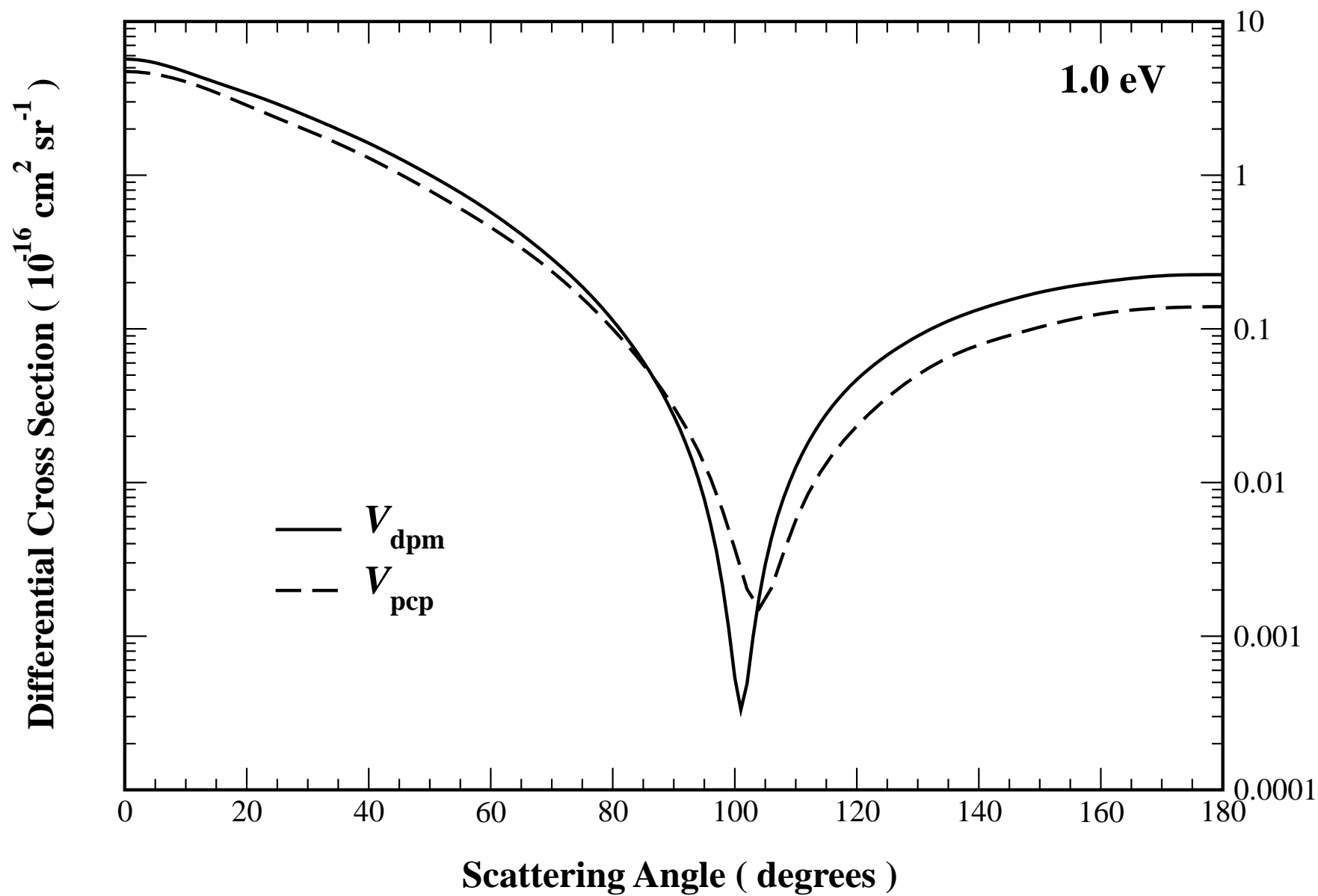


Figure 3

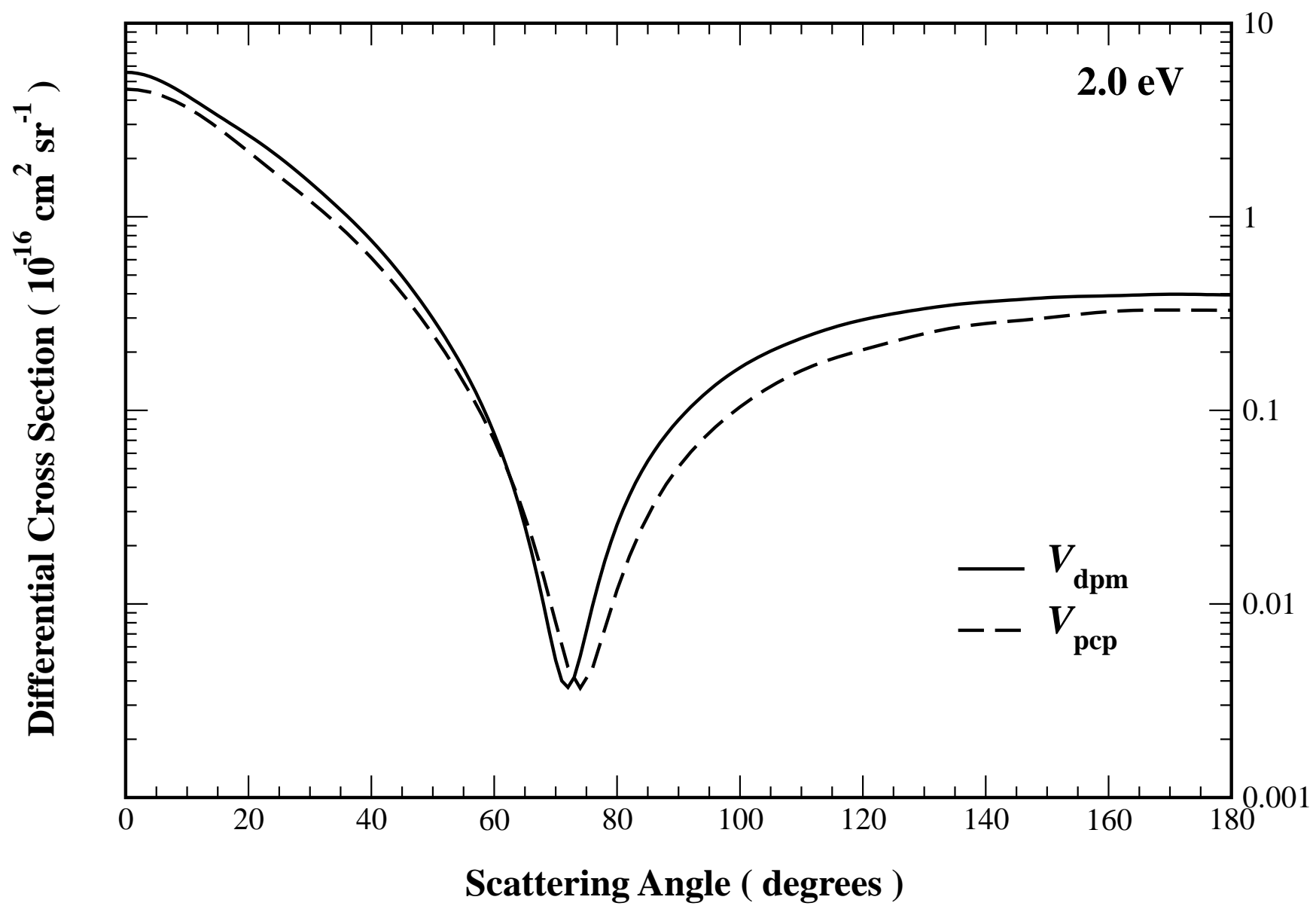


Figure 4

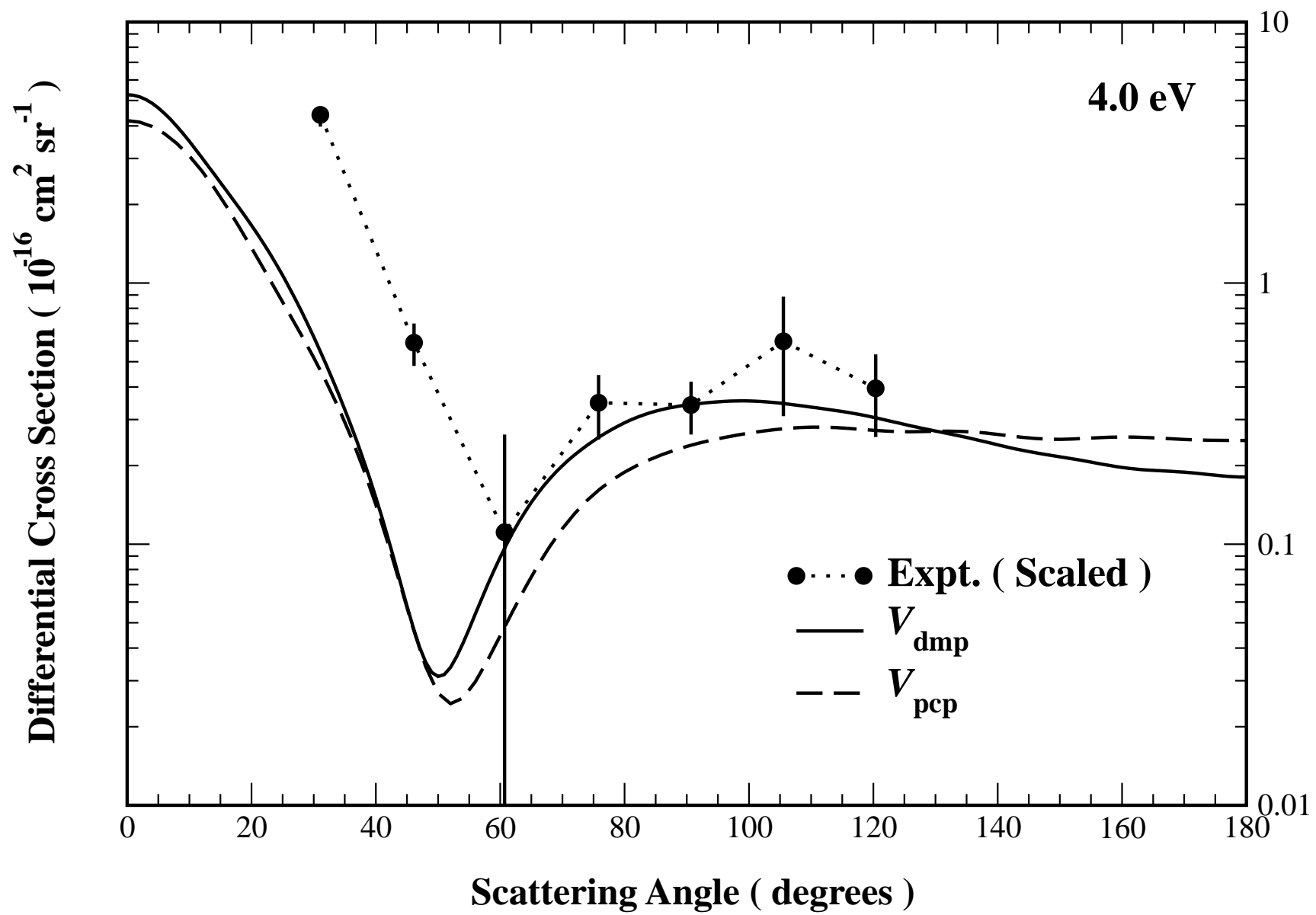


Figure 5

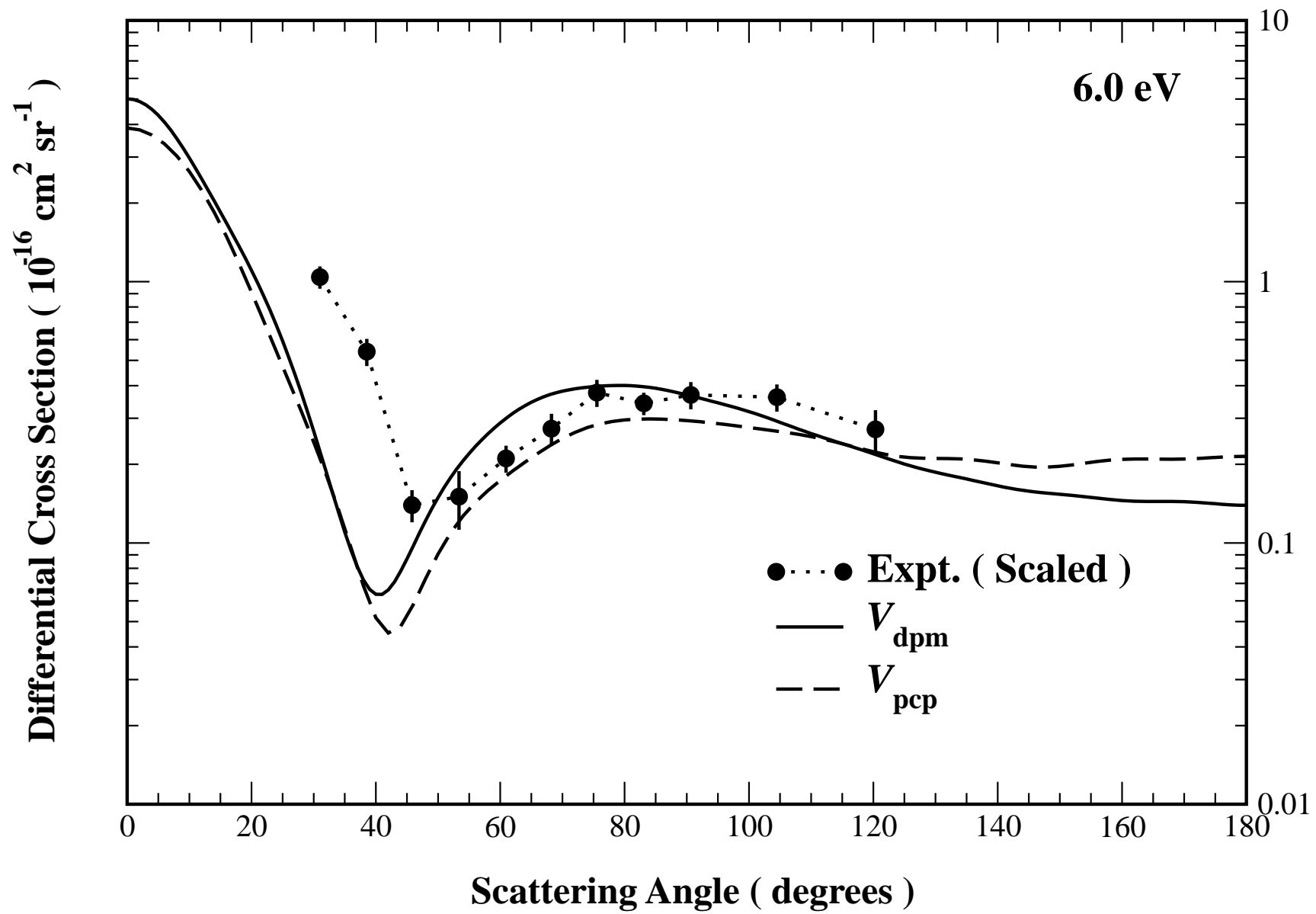


Figure 6